doi:10.3788/gzxb20174602.0229002

用于校准能见度仪的标准散射体定标系统中光学系统的误差分析

张健[1],张国玉[1,2,3],张建良[4],赵云率[1]

(1 长春理工大学,长春 130022)

(2 光电测控与光电信息传输技术教育部重点实验室,长春,130022)

(3 吉林省光电测控仪器工程技术研究中心,长春 130022)

(4 空军航空大学,长春 130022)

摘 要:为了实现用于校准能见度仪的标准散射体的快速高精度定标,依据标准散射体校准前向散射式能见度仪的校准原理,建立定标系统中光学系统的误差分析方法.分析标准散射体定标系统的工作原理,结合其光学系统、机械结构的加工及装调偏差,建立了标准散射体定标系统的光学系统模型并设计实验证明其正确性.分析影响定标系统中光学系统精度的主要误差,得到标准散射体定标系统中光学系统的误差传递模型.通过对畸变偏差、像面位置偏差、主点位置偏差、像面倾斜偏差和焦距偏差的分析,提出了一种系统综合误差分析的方法并建立了综合偏差模型,对每个偏差单独分析,得出畸变偏差、像面位置偏差、主点位置偏差、像面倾斜偏差和焦距偏差的偏差范围依次为0.024 mm,0.399 mm,0.02 mm,0.28 rad和0.392 mm.该研究为提高用于校准能见度仪的标准散射体定标系统的精度以及校准时误差的来源分析与补偿提供理论依据.

关键词:能见度与成像;像差补偿;光学设计及装配;校准;气象仪器

中图分类号:TH765.8+3 **文献标识码**:A **文章编号**:1004-4213(2017)02-0229002-12

Optical System Error Analysis for Standard Scattering Plate Calibration System Used in Calibration Visibility Meter

ZHANG Jian[1], ZHANG Guo-yu[1,2,3], ZHANG Jian-liang[4], ZHAO Yun-shuai[1]

(1 *Changchun University of Science and Technology, Changchun* 130022, *China*)

(2 *Key Laboratory of Optical Control and Optical Information Transmission Technology, Department of Education, Changchun* 130022, *China*)

(3 *Optical Measurement and Control Instrumentation, Jilin Province Engineering Research Center, Changchun* 130022, *China*)

(4 *Aviation University of Air Force, Changchun* 130022, *China*)

Abstract: In order to realize the rapid and high precision calibration of standard scattering plate used in calibrating visibility meter, based on the calibration principle which a standard scattering plate calibrates a forward scattering visibility meter, an error analysis method for the optical system of the standard scattering plate calibration system used in a calibration visibility meter was established. The working principles of the calibration system were analyzed, and subsequently, a model of this optical system was

Foundation item: The National Public Welfare Industry Science and Technology Projects in China (Nos. GYHY200706003, GYHY201006043)

First author: ZHANG Jian (1989—), male, Ph. D. candidate, mainly focuses on meteorological instruments, photoelectric instrument and testing technology. Email: zhangjian_nr@126.com

Supervisor: ZHANG Guo-yu (1962—), male, professor, Ph. D. degree, mainly focuses on space science and technology, photoelectric instrument and testing technology. Email: zh_guoyu@163.com

Received: Sep. 21, 2016; **Accepted**: Dec. 6, 2016

established with a combination of the deviation arising from its optical system, fabrication and adjustment. Further, an experiment was designed to validate the model's correctness. Next, the main errors that affect the precision of the scattering plate's optical system were analyzed, for which an error propagation model was constructed. Finally, a comprehensive error analysis method for the system is proposed and a comprehensive deviation model is developed according to the analysis of the deviation of distortion, image plane position, principal point position, image plane inclination, and focal length. Each deviation is analyzed respectively, and the allowable deviation range of the deviation of distortion, image plane position, principal point position, image plane inclination, and focal length are, in order, 0.024 mm, 0.399 mm, 0.02 mm, 0.28 rad and 0.392 mm. Consequently, there is theoretical basis for precision improvement of the calibration system and the error sources analysis and compensation during calibration.

Key words: Visibility and imaging; Aberration compensation; Optical design and fabrication; Calibration; Meteorological instrument

OCIS Codes: 290.1310;010.7295;220.1000;220.0220;150.1488

0 Introduction

Atmospheric horizontal visibility, which is an important physical quantity that represents the atmosphere pollution degree of the subsurface, has a great influence on the aviation, navigation, transportation and military actions. The main instruments for visibility measurement are transmission type visibility meter, forward scattering type visibility meter, backward scattering type visibility meter, Digital Photography Visiometer System (DPVS) and laser radar. On account of the convenience of installation, usage and maintenance for the forward scattering type visibility meter, it has been widely used. At present, standard transmission type visibility meters or standard scattering plates are mainly utilized for calibration of a forward scattering type visibility meter, so the calibration precision of the standard transmission type visibility meter and standard scattering plate determines the calibration accuracy of the forward scattering type visibility meter. The calibration accuracy of using a transmission type visibility meter is high. However, the price of a transmission type visibility meter is very expensive, and it is hard to calibrate. It also would take a long time to adjust and be easily influenced by the environment factors. At the same time, it could only be used for out-field calibration. Compared to it, the calibration method of using a standard scattering plate could be used for both infield and out-field calibration. And its calibration method is easy. With shorter calibration time and low cost, so the standard scattering plate is currently widely used to calibrate forward scattering type visibility meters.

There are some related research on how to use standard scattering plates to calibrate a forward scattering type visibility meter. Wang Qing-mei et al proposed a project assumption on using a calibrated forward scattering type visibility meter to produce a series of calibrated plates to calibrate the forward scattering type visibility meter at work site[1]. Zhu Le-qun et al proposed the condition and method of lab calibration of forward scattering type visibility meter, summed up and sorted out the methods of optical device calibration at wok site, calibrated plate calibration, and manual calibration[2]. Cheng Yin et al proposed to use a scattering plate and an attenuation plate with different transmittances to simulate several standard measured points of the forward scattering type visibility meter to correct the modifier formulas of the visibility meter for calibrating the forward scattering type visibility meter[3]. Wang Mian et al used two scattering plates with the same transmittance coefficient to calibrate the forward scattering type visibility meter[4]. At present, in the foreign, the calibration method of standard scattering plate used in a calibration visibility meter is mainly the calibration method for the standard scattering plate in the Vaisala FD12P calibration method which was put forward by Royal Netherlands Meteorological Institute (KNMI)[5]. The calibration method could be divided into four steps. Step 1: Utilizing a neutral density filter to calibrate a transmission type visibility meter; step 2: Utilizing a standard scattering plate to calibrate a forward scattering type visibility meter; step 3: Comparing the observation data of the previous two sets of calibrated transmission type visibility meters and calibrated forward scattering type visibility meter; step 4: Correcting of the scattering coefficient of the standard scattering plate in the set 3. The calibration method could trace back to the

marked transmittance accuracy of a neutral density filter in the laboratory. The standard scattering plate of the forward scattering type visibility meter utilizes its scattering coefficient to simulate the corresponding visibility conditions. With the rapid development of the measurement of bi-directional scattering distribution function, it realizes calibration by measuring the scattering coefficient of the standard scattering plate[6-15].

The standard scattering plate calibration system used in calibration visibility meters is a new type of calibration system for the standard scattering plate that is utilized for the calibration of forward scattering type visibility meters. The precision of the standard scattering plate calibration system used in calibration visibility meters is dependent on the imaging quality of its optical system and calibration accuracy of the system. An optical system with enhanced imaging quality can provide a good foundation for calibration, data collection, and analysis of the system, which is beneficial to improving the detection precision of the calibration system. Further, research on the error sources affecting the optical system precision becomes essential. Moreover, it is also important to develop analytical methods of precision in order to obtain a comprehensive and visualized error propagation model for calibration and compensation of error. Such research can significantly improves the precision of a standard scattering plate calibration system used in calibration visibility meters.

In this study, we analyze the working principles of a standard scattering plate calibration system used in a calibration visibility meter. Then, with a combination of the deviation arising from imperfections in fabrication and physical adjustment of the optical system, we establish a working model for the optical system of the calibration visibility meter and design an experiment to validate its correctness. After that, we analyze the main error sources that affect the precision of its optical system, and we develop an error propagation model for this optical system. We also propose a comprehensive error analysis method for the system according to our analysis on the deviations of distortion, image plane position, principal point position, image plane inclination, and focal length. The precision index of the standard scattering plate calibration system determines the allowable deviation range of each individual deviation and we obtain the allowable deviation range and examine how the calibration system precision varies as a function of this range along with variation in the field angles of the calibration system. Laboratory calibration can further be realized on the basis of these limitation requirements in order to develop the theoretical basis for precision improvement of the standard scattering plate calibration system.

1 The composition and working principle of calibration system

1.1 The calibrating principle of using a standard scattering plate to calibrate a forward scattering type visibility meter

The definition of meteorology for visibility is that the maximum distance which the eyes with standard vision can distinguish the black body targets contour from the background of sky on the horizontal direction[16]. The results of visibility measured by human eyes are always different, due to the difference of awareness, resolving power and light source characteristics. In order to define the visibility objectively, World Meteorological Organization (WMO) proposed to use atmospheric transparency to evaluate the visibility in 1957. Visibility expressed as Meteorological Optical Range (MOR), and definition of MOR is the distance which luminous flux of parallel light exited from the incandescent light bulb under the condition that color temperature of 2700k is attenuated to the 5% of the initial luminous flux[17].

According to the Koschmieder's law[18], when black body targets are on the background of sky, the contrast between the apparent brightness of the targets and the background can be expressed as

$$R_m = \frac{1}{\sigma} \ln \frac{1}{\varepsilon} \tag{1}$$

In the Eq. (1), R_m is weather range of visibility, ε is contrast threshold of human vision, σ is atmospheric extinction coefficient.

Atmospheric extinction coefficient σ is the sum of scattering coefficient K_s and absorption coefficient K_a. The absorption effect of atmospheric aerosol is much less than the scattering effect of atmospheric aerosol. According to provisions of the WMO, the visibility V can be expressed as

$$V = \frac{-\ln \varepsilon}{K_s} \tag{2}$$

Based on the Mie scattering theory[19], when the range of scattering angle θ of atmospheric aerosol is between 20°and 50°, the relationship among scattered light intensity $I(\theta)$, scattering coefficient K_s, and incident intensity I_0 can be expressed as[20]

$$I(\theta)=K_s I_0 \tag{3}$$

According to the Eqs. (2) and (3), forward scattering type visibility meter can measure the visibility V indirectly by measuring the scattering coefficient K_s, and the standard scattering plate can simulate the different visibility V by simulating different scattering coefficients K_s to calibrate the forward scattering type visibility meter.

1.2 The composition and working principle of calibration system

According to the Eqs. (2) and (3), when $\varepsilon=0.05$, the relationship among scattered light intensity $I(\theta)$, visibility V, and incident intensity I_0 can be expressed as

$$V=\frac{2.996 I_0}{I(\theta)}=\frac{2.996}{I(\theta)/I_0} \tag{4}$$

Based on the Eq (4), only if a standard scattering plate calibration system used in calibration visibility meter can measure the scattered light intensity $I(\theta)$ and the incident intensity I_0 of scattering angle θ, can the visibility V which is simulated by the standard scatter plate be measured.

The optical system for the calibration system of the standard scatterer used in a visibility meter is consisted of an illuminating system and a paraboloid catadioptric optical system. Thereinto, the paraboloid catadioptric optical system is consisted of a paraboloid reflector and the optical system of the imaging colorimeter[21]. The system composition is shown in Fig. 1.

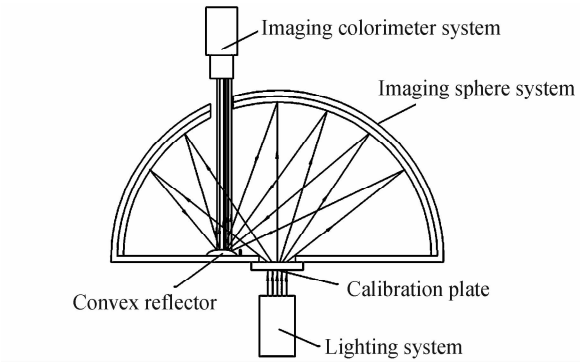

Fig. 1 System composition

The light beams emitted from the illuminating system scatter on the inner surface of the imaging sphere after they shine uniformly and penetrate the standard scatterer, and form the optical field distribution in the inner surface of the imaging sphere after scattered by the standard scatterer. The field of view of the imaging colorimeter optical system is enlarged by the parabolic reflector, thus realizing the collection of the energy distribution of the inner wall of the entire imaging sphere. The scattering coefficient of the standard scatterer in each scattering angle is obtained through the software. The visibility simulated by the standard scatting plate can be calibrated.

1.3 Optical system model for standard scattering plate calibration system

The optical system of the standard scattering plate calibration system used in a calibration visibility meter is a catadioptric imaging system consisting of a convex reflector in the imaging sphere system and the imaging colorimeter optical system[22]. The convex reflector enlarges the field of the imaging colorimeter optical system. Thus, the illuminance distribution within the entire imaging sphere is collected. For the standard scattering plate calibration system used in calibration visibility meters, the use of a paraboloid catadioptric system enables easy adjustment and calibration; the distance between the reflector and CCD can be easily adjusted, which makes the system become an ideal catadioptric panorama model. Consequently, we apply a paraboloid reflecting-mirror plane-type system in our study. The optical model of the system is shown in Fig. 2. In the figure, α_1 and α_2 represent the incident angle of incident ray 1 and incident ray 2.

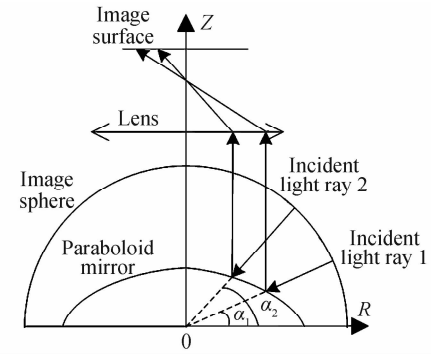

Fig. 2 Optical model of the system

We utilize two rotating platforms, a laser, and a parabolic reflector to set up a test platform, as shown in Fig. 3, in order to validate the correctness of the abovementioned optical model of the system.

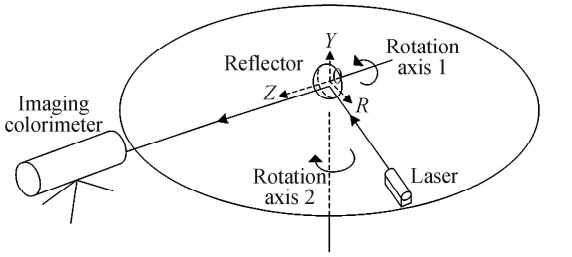

Fig. 3 Schematic of test platform

In Fig. 3, rotation axis 1 drives the reflector to rotate around the *Z*- axis with the reflector center being the center of rotation; rotation axis 2 drives the laser to rotate around the *Y*-axis with the reflector center being the center of rotation. The light emitted by the laser enters the imaging colorimeter after reflection from the reflector. This setup can be used to simulate the illuminating conditions of any point of the reflector, and further simulate the in-wall imaging conditions within the entire imaging sphere as collected by the imaging colorimeter via the rotation of the laser and the reflector. Furthermore, we can validate the correctness of the optical model of the system.

We simulate the conditions of the incident angle within the range of 0° - 180° in the *ROZ* plane via individual control of the laser rotation. Next, we carry out an experiment via light sampling at every 20°-step. In a similar manner, we simulate the conditions of the incident angle within the range of 0° - 360° in the *ROY* plane via individual control of the reflector's rotation. Subsequently, we carry out an experiment via sampling at every 20°-step. The test results are shown in Fig. 4 and Fig. 5.

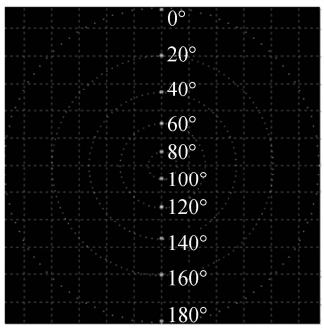

Fig. 4 Laser rotation sampling output

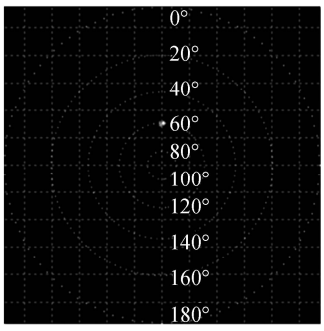

Fig. 5 Reflector rotation sampling output

From Fig. 4, we note that as the incident angle varies from 0° to 180°, the movement locus of the laser spots collected by the receiving surface of the imaging colorimeter is a straight line. Moreover, the direct interval of the spot corresponding to each sampling is centrally symmetrical to the image surface. This result indicates that the optical system of the calibration system is axially symmetrical with respect to the *Y*-axis. Further, from Fig. 5, we note that as the incident angle varies from 0° to 360°, the movement locus of the laser spots collected by the receiving surface of the imaging colorimeter is an approximate single point or dot. This result indicates that the optical system of the calibration system is rotationally

symmetrical with respect to the Z-axis. Consequently, we can validate the correctness of the optical model of the system.

2 Error propagation model of the entire system

The standard scattering plate calibration system uses a CCD, which is positioned in the image plane, and the paraboloid reflector and the optical system of an imaging colorimeter are utilized to collect light energy from all angles of the inner wall within the imaging sphere in order to obtain the optical field distribution within the imaging sphere. We analyze the imaging colorimeter optical system and convex reflector in the imaging sphere of the system as below.

2.1 Error propagation model for imaging colorimeter

From Fig. 2, it can be inferred that the ideal model for the optical system of the imaging colorimeter is a pinhole imaging model, which is shown in Fig. 6.

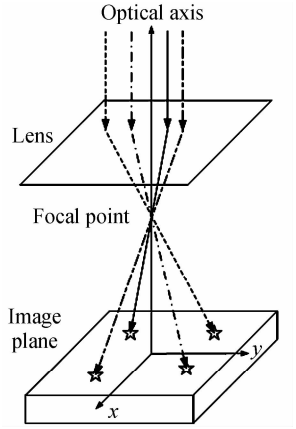

Fig. 6 Ideal model for the optical system of an imaging colorimeter

In reality, the ideal pinhole imaging model cannot be realized because of the optical aberration of the imaging colorimeter optical model, fabrication errors in the machining precision and its adjustment, and other deviations [23-24]. Consequently, the optical field distribution within the imaging sphere collected by the CCD is affected in the practical case. Further, the chromatic aberration of the optical system of the imaging colorimeter and monochromatic aberration (except for distortion) affect the degrees, dimensions, and colors of the image at the inner wall of the imaging sphere, which is imaged through the optical system onto the CCD[25]. These abovementioned factors can significantly influence the accurate mapping of the intensity and angles for CCD detection. Therefore, the imaging colorimeter must be rigorously calibrated during the optical system design. According to the ideal optical model of the imaging colorimeter, we can conclude that the deviation of the image plane position, principal point position, image plane inclination, and focal length occur along the image plane due to defects arising from the mechanical structure during fabrication and adjustment during actual operation.

The models for distortion deviation, image plane positional deviation, principal point deviation, image plane inclination deviation, and focal length deviation are shown in Figs. 7, 8, 9, 10, and 11, respectively. The factors that affect the precision of the imaging colorimeter are mainly the distortion deviation ΔD, image plane position deviation ΔH, principal point deviation ΔP, image plane inclination deviation $\Delta\theta$, and focal length deviation ΔF. F denotes the lens focal length, f is the distance between the image plane and the focus, m is the ideal object height, and M is the distance between the incidence point of the ideal light ray on the prism and the optical axis. I_D, I_H, I_P, I_θ and IF denote the actual object height of each model respectively. L_D, L_H, L_P, L_θ and L_F denotes the distance between the incidence point of the actual light ray on the prism and the optical axis of each model respectively. The deviation of distortion, image plane position, principal point, image plane inclination, focal length are expressed as Eq. (5)～Eq. (9) below respectively

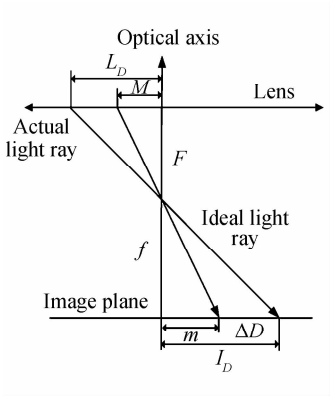

Fig. 7 Model for distortion deviation

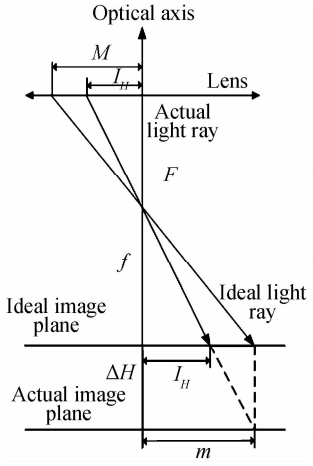

Fig. 8 Model for image plane positional deviation

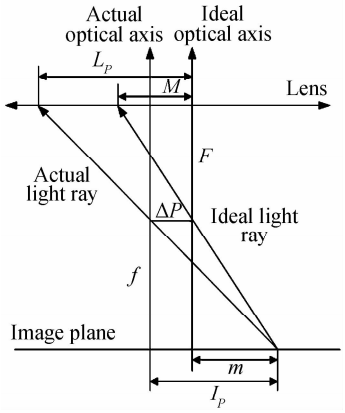

Fig. 9 Model for principal point positional deviation

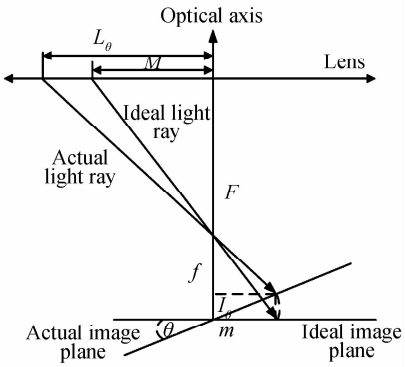

Fig. 10 Model for image plane inclination deviation

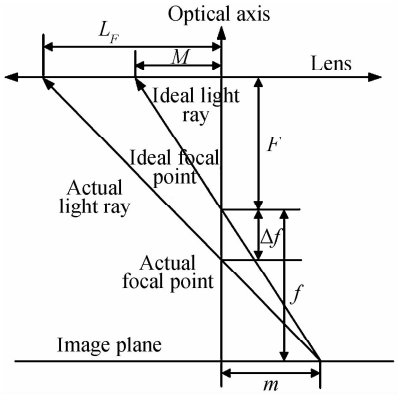

Fig. 11 Model for focal length deviation

$$\mathrm{Error}_D=(L_D-M)=\frac{F}{f}\cdot(m+\Delta D)-M \tag{5}$$

$$\mathrm{Error}_H=(L_H-M)=\frac{F}{f}\cdot\frac{m\cdot f}{f+\Delta H}-M \tag{6}$$

$$\mathrm{Error}_P=(L_P-M)=\frac{F+f}{f}\cdot\Delta P \tag{7}$$

$$\mathrm{Error}_\theta=(L_\theta-M)=\frac{m\cdot\cos\theta\cdot F}{f-m\cdot\sin\theta}-M \tag{8}$$

$$\mathrm{Error}_f=(L_F-M)=\frac{m\cdot(F+\Delta f)}{f-\Delta f}-M \tag{9}$$

The factors that affect the precision of the imaging colorimeter are mainly the distortion deviation ΔD, image plane position deviation ΔH, principal point deviation ΔP, image plane inclination deviation $\Delta\theta$, and focal length deviation ΔF. Taking a certain fixed point on the image plane as an example, we can establish a comprehensive deviation model (Fig. 12) that considers all the various deviations that a light ray on the

image plane can undergo. In Fig. 12, F denotes the lens focal length, f is the distance between the image plane and the focus, m is the ideal object height, and M is the distance between the incidence point of the ideal light ray on the prism and the optical axis. A total of 6 light rays can be observed in the figure: Light rays from No. 1 to No. 6 are the ideal light ray, actual light ray subject to deviation of distortion and image plane position; actual light ray subject to distortion deviation; actual light ray subject to deviation of distortion, image plane position, and principal point; actual light ray with deviation of distortion, image plane position, principal point, and focal length; and actual light ray with the deviation of distortion, image plane position, principal point, image plane inclination, and focal length.

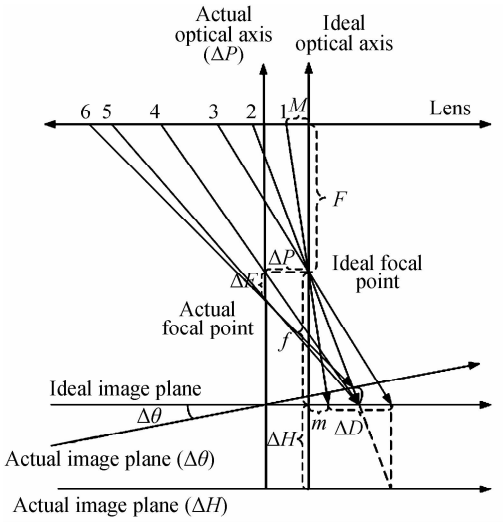

Fig. 12 Comprehensive deviation model

We can deduce the deviation between an ideal light ray and the corresponding actual light ray subject to deviation of distortion, image plane position, principal point, image plane inclination, and focal length according to the models from Fig. 7 to Fig. 12. This deviation is the comprehensive deviation of the imaging colorimeter, which is expressed as

$$\mathrm{Error}=\frac{\cos\theta\cdot(F+\Delta f)\cdot\left(\Delta P+\frac{(m+\Delta D)\cdot f}{f+\Delta H}\right)}{(f-\Delta f)-\sin\theta\cdot\left(\Delta P+\frac{(m+\Delta D)\cdot f}{f+\Delta H}\right)}-M \tag{10}$$

2.2 Error propagation model for convex reflector within imaging sphere

From Fig. 2, as regards the optical system of the imaging colorimeter, the overall deviation finally affects the incident light position on the principal plane of the optical system. Therefore, it is required to establish an error propagation model for the convex reflector within the imaging sphere. We can deduce the angular deviation of the in-wall energy distribution of the imaging sphere detected by the calibration system according to the deviation of the imaging colorimeter. The error propagation model for the convex reflector

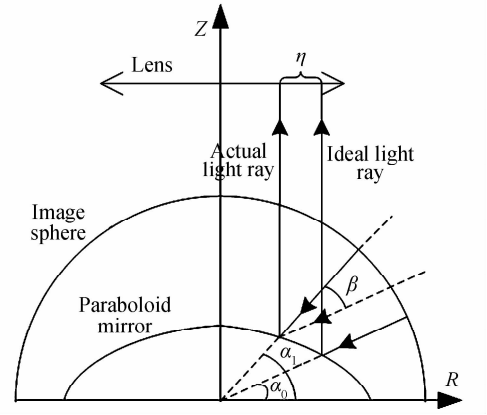

Fig. 13 Error propagation model for convex reflector within imaging sphere

within the imaging sphere is shown in Fig. 13. In the figure, η represents the comprehensive deviation of the imaging colorimeter, α_0 represents the incident angle of the ideal light ray, α_1 represents the incident angle of the corresponding actual light ray, and β represents the angular deviation.

From Fig. 13, disregarding the off-axis deviation of the convex reflector and other deviations, for known values of the reflecting-mirror plane-type function $z(r)$, the allowable incident light angle range σ of the reflector, and angular resolution γ of the imaging sphere in-wall required by the system, we can obtain the range of the allowable comprehensive deviation η of the imaging colorimeter under the condition of satisfying the detected resolution γ of the system.

3 Error analysis and simulation

A standard scattering plate calibration system with an angular resolution of $\gamma=1°$, as designed in the study, is adopted as the object of analysis. The dimensions of the optical sensor of the imaging colorimeter are 1 024 px×1 024 px. The physical dimensions of each pixel are 5.5 μm×5.5 μm, and the image plane dimensions are 5.6 mm×5.6 mm. The object height is 25 mm and object distance is 451.09. Moreover, the convex reflector function $f(x)$ within the imaging sphere is expressed as $r^2=-25z+\frac{625}{4}$. The angular range of the incident light on the reflector is $\sigma \in [0°, 90°]$.

Exploiting the relationship between the paraboloid equation and the incident light angle, we have

$$\begin{cases} r^2=-25z+\dfrac{625}{4} \\ \dfrac{z}{r}=\tan\alpha (0°\leqslant\alpha\leqslant 90°) \end{cases} \tag{11}$$

From Eq. (11), the allowable maximum comprehensive deviation η of the imaging colorimeter of the system is 0.109 mm in our case. In this regard, the plot of "r" as a function of "α" is shown in Fig. 14.

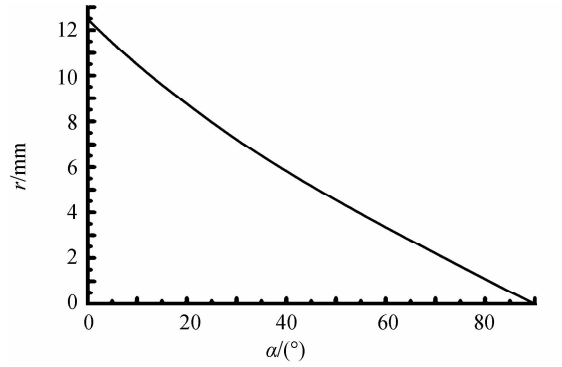

Fig. 14 Variation in "r" as a function of "α"

According to the error propagation model of the system, we can utilize the method of maximum error. We individually analyze each deviation in order to obtain the position of the maximum error point or a given angular resolution of the system. The deviations and distribution of different angles of incidence can be intuitively derived, which can further aid future studies in this direction.

3.1 Effects of distortion deviation on angular resolution of system

For a given angular resolution of the system, the allowable maximum distortion deviation ΔD is 0.024 mm. The effect of the distortion deviation on the angular resolution precision of the system and incident angle is shown in Fig. 15.

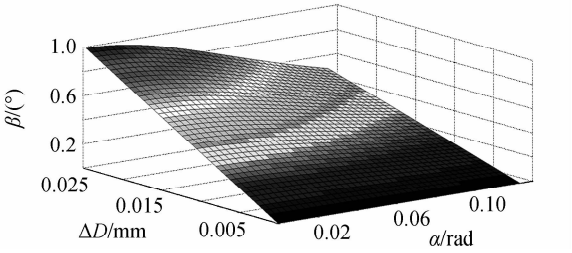

Fig. 15 Effects of distortion deviation on the angular resolution precision of the system

From the figure, we observe that the angular detection deviation of the calibration system increases with increase in the distortion deviation, and the distortion deviation strongly influences the angular detection precision for a small field range of the calibration system.

3.2 Effects of image plane positional deviation on angular resolution of the system

For a given angular resolution of the system, the maximum allowable image plane positional deviation ΔH is 0.399 mm. The effect of variation in the image plane positional deviation on the angular resolution precision of the system and incident angle is shown in Fig. 16.

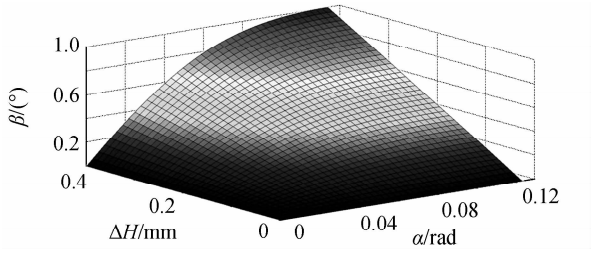

Fig. 16 Effects of image plane positional deviation on the angular resolution precision of the system

From the figure, we observe that the angular detection deviation of the calibration system increases with increase in the image plane positional deviation. Further, the influence of the image plane positional deviation on the angular detection precision of the calibration system increases with increase in the field angle.

3.3 Effects of principal point positional deviation on angular resolution of the system

For a given angular resolution of the system, the maximum allowable principal point positional deviation ΔP is 0.02 mm. The effect of variation in the principal point positional deviation on the angular resolution precision of the system and incident angle is shown in Fig. 17.

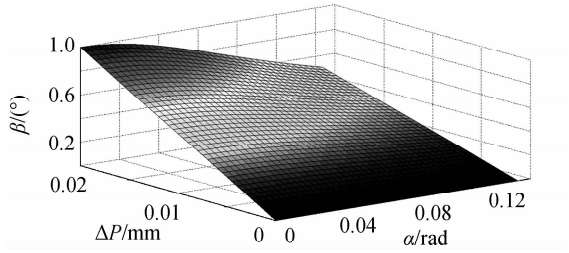

Fig. 17 Effects of principal point positional deviation on the angular resolution precision of the system

From the figure, we note that the angular detection deviation of the calibration system increases with increase in the principal point positional deviation, and the influence of the principal point positional deviation on the angular detection precision of the calibration system decreases with increase in the field angle.

3.4 Effects of image plane inclination deviation on angular resolution of the system

For a specified angular resolution of the system, the maximum allowable image plane inclination deviation $\Delta\theta$ is 0.28 rad. The effect of variation in the image plane inclination deviation on the angular resolution precision of the system and incident angle is shown in Fig. 18.

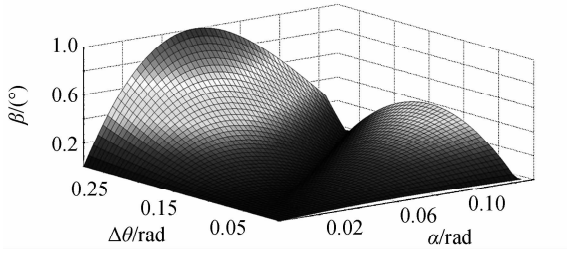

Fig. 18 Effects of image plane inclination deviation on the angular resolution precision of the system

From the figure, we observe that the angular detection deviation of the calibration system exhibits an increase-decrease-increase trend with the increase in image plane inclination deviation. Futhermore, the influence of image plane inclination deviation on the angular detection precision of the calibration system exhibits an increase-decrease-increase trend with the increase in the field angle.

3.5 Effects of focal length deviation on the angular resolution of the system

For a specified angular resolution of the system, the maximum allowable focal length deviation ΔF is 0.392 mm. The effect of variation in the focal length deviation on the angular resolution precision of the system and incident angle is shown in Fig. 19.

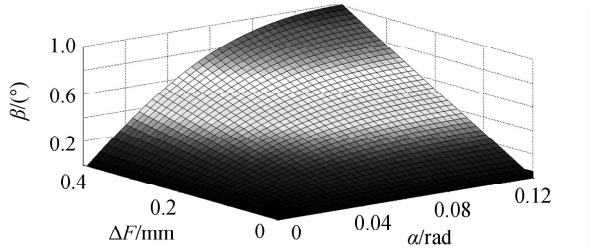

Fig. 19 Effects of focal length deviation on the angular resolution precision of the system

From the figure, we note that the angular detection deviation of the calibration system increases with the increase in the focal length deviation, and the influence of the focal length deviation on the angular detection precision of the calibration system increases with the increase in the field angle.

Table 1 lists the simulation results for the maximum allowable deviation values of the deviation of distortion, image plane position, principal point, image plane inclination, and focal length as well as the extent to which the field angle area is affected.

Table 1 Maximal allowable deviation values of the deviation of distortion, image plane position, principal point, image plane inclination, and focal length

Deviation type	Maximum allowable value	Effective field angle area
Distortion deviation	0.024 mm	Small field of view
Image plane positional deviation	0.399 mm	Large field of view
Principal point deviation	0.02 mm	Small field of view
Image plane inclination deviation	0.28 rad	Middle field of view
Focal length deviation	0.392 mm	Large field of view

From these results, it can be concluded that in order to ensure that the imaging colorimeter optical system meets the angular resolution of the standard scattering plate calibration system without further calibration, and the distortion deviation and principal point deviation are important calibration subjects for the system within the range of a small field of view. However, the image plane positional deviation and focal length deviation can be calibrated within the range of a large field of view. Because of the complexity arising in the case of the image plane inclination deviation (making it difficult for calibration), we emphasize on taking the calibration and compensation of the image plane inclination deviation into consideration when designing the optical structure of the calibration system. The angular resolution precision of the system can be further improved by means of follow-up calibration tests and sub-pixel extraction techniques.

4 Conclusion

Via a study of error analysis methods for the optical system of a standard scattering plate calibration system used in a calibration visibility meter, we constructed an optical model of the calibration system and designed an experiment to validate its correctness. Subsequently, we obtained an error propagation model in accordance with the optical model analysis of the calibration system. Next, we analyzed certain important factors (distortion deviation, image plane positional deviation, principal point deviation, image plane inclination deviation, and focal length deviation) that affect the precision of the optical system of the calibration visibility meter according to the index of the standard scattering plate calibration system. With our approach, we can obtain the allowable deviation range of each individual deviation and the impact trend of variation in the field angle on the calibration system precision for a given system index. Consequently, the approach can provide a theoretical basis for the proposal and demonstration of the design index for this optical system along with analysis of the main error sources and their compensation in the optical system during the calibration and correction processes of the calibration system.

References

[1] WANG Qing-mei, XIE Bang-li, MEI Pin-chen, *et al*. Discussing the theory and calibration of the forward scaffer metter [J]. *Meteorological, Hydrological and Marine Instrument*, 2001,(4):10-16.

[2] ZHU Le-kun, LI Lin. Calibration technology of forward scattering visibility metters[J]. *Meteorological Science and Technology*, 2013, **41**(6):1003-1007.

[3] CHEN Yin. A calibration method of forward scattering type visibility meter: China, 103278478 A[P]. 2013-09-04.

[4] WANG Mian, LIU Wen-qing, LU Yi-Huai, *et al*. Calibration and correction methods for the transform coefficients of the atmospheric visibility system by aerosol forward-scattering theory[J]. *Optical Technique*, 2008, **34**(3):334-337.

[5] BLOEMINK H I. KNMI visibility standard for calibration of scatterometers[C]. 4th ICEAWS International Conference on Experiences with Automatic Weather Stations, Lisboa, Portugal. 2006.

[6] BARTELL F O, DERENIAK E L, WOLFE W L. The theory and measurement of bidirectional reflectance distribution function /BRDF/ and bidirectional transmittance distribution function /BTDF/[C]. SPIE, 1980, **257**:154-160.

[7] STUHLINGER T W, DERENIAK E L, BARTELL F O. Bidirectional reflectance distribution function of gold-plated sandpaper[J]. *Applied Optics*, 1981, **20**(15):2648-55.

[8] DAVIS L, KEPROS J G. Improved facility For BRDF/BTDF optical scatter measurements[C]. SPIE, 1986, **675**:24-32.

[9] CADY F M, STOVER J C, BJORK D R, *et al*. Design review of a multiwavelength, three-dimensional scatterometer [C]. San Dieg - DL Tentative. International Society for Optics and Photonics, 1990.

[10] DROLEN B L. Bidirectional reflectance and surface specularity results for a variety of spacecraft thermal control materials[C]. 26th Thermophysics Conference Honolulu, HI, USA. 1991.

[11] MIETTINEN J, HARKONEN A K, PIIRONEN T H. Optical scattering measurement instrument for the design of machine vision illumination[C]. SPIE, 1992, **1614**:45-56.

[12] TSUCHIDA S, SATO I, OKADA S. Measurement of land surface BRDF with spatial instability for vicarious calibration[C]. Sensors, Systems, and Next-Generation Satellites III. Sensors, Systems, and Next-Generation Satellites III, 1999.

[13] KLAASSEN T O, SMORENBURG K. Reflectance measurements on submillimeter absorbing coatings for HIFI[C]. SPIE, 2000, **4013**:129-139.

[14] DANA K J. BRDF/BTF measurement device[C]. Computer Vision, 2001. Eighth IEEE International Conference on ICCV 2001. 2001,**2**:460-466.

[15] WADMAN S, BAUMER S. Appearance characterization by a scatterometer employing a hemispherical screen[C]. SPIE, 2003,**5189**:163-173.

[16] LI Chun-liang. Hundred questions of visibility measurement technique[M]. China Meteorological Press, 2009.

[17] WMO G. WMO guide to meteorological instruments and methods of observation. WMO-No. 8[M]. Secretariat of the World Meteorological Organization, 1983, I9-1.

[18] ZHANG Cheng-chang. A course of atmospheric aerosol[M]. China Meteorological Press, 1995.

[19] ZHOU Xiu-ji. Advanced atmospheric physics[M]. China Meteorological Press, 1991.

[20] YU Rong-bin. A research on testing theory and technology improving forward direction light scattering of small angle [D]. South China Normal University, 2002.

[21] RYKOWSKI R, CHITTIM K, WADMAN S. Imaging sphere enables rapid source, intensity mapping[J]. *Photonics Spectra*, 2005, **399**:64-69.

[22] CHAHL J S, SRINIVASAN M V. Reflective surfaces for panoramic imaging[J]. *Applied Optics*, 1997, **36**(31): 8275-8285.

[23] XING F, DONG Y, ZHENG Y. Laboratory calibration of star tracker with brightness independent star identification strategy[J]. *Optical Engineering*, 2006, **45**(6):711-725.

[24] SUN T, XING F, YOU Z. Optical system error analysis of high accuracy star trackers[J]. *Acta Optica Sinica*, 2013, **33**(3):253-261.

[25] ZOU Y, ZHANG G, SUN G, *et al*. Star position correction of dynamic star simulator based on distortion effect[J]. *Chinese Journal of Space Science*, 2014, **34**(4):468-473.